LBNL-47349
Preprint

ERNEST ORLANDO LAWRENCE
BERKELEY NATIONAL LABORATORY

McMillan-Mayer Solution Thermodynamics for a Protein in a Mixed Solvent

R.A. Curtis, J. Newman, H.W. Blanch,
and J.M. Prausnitz

Chemical Sciences Division

January 2001

Submitted to
Fluid Phase Equilibrium

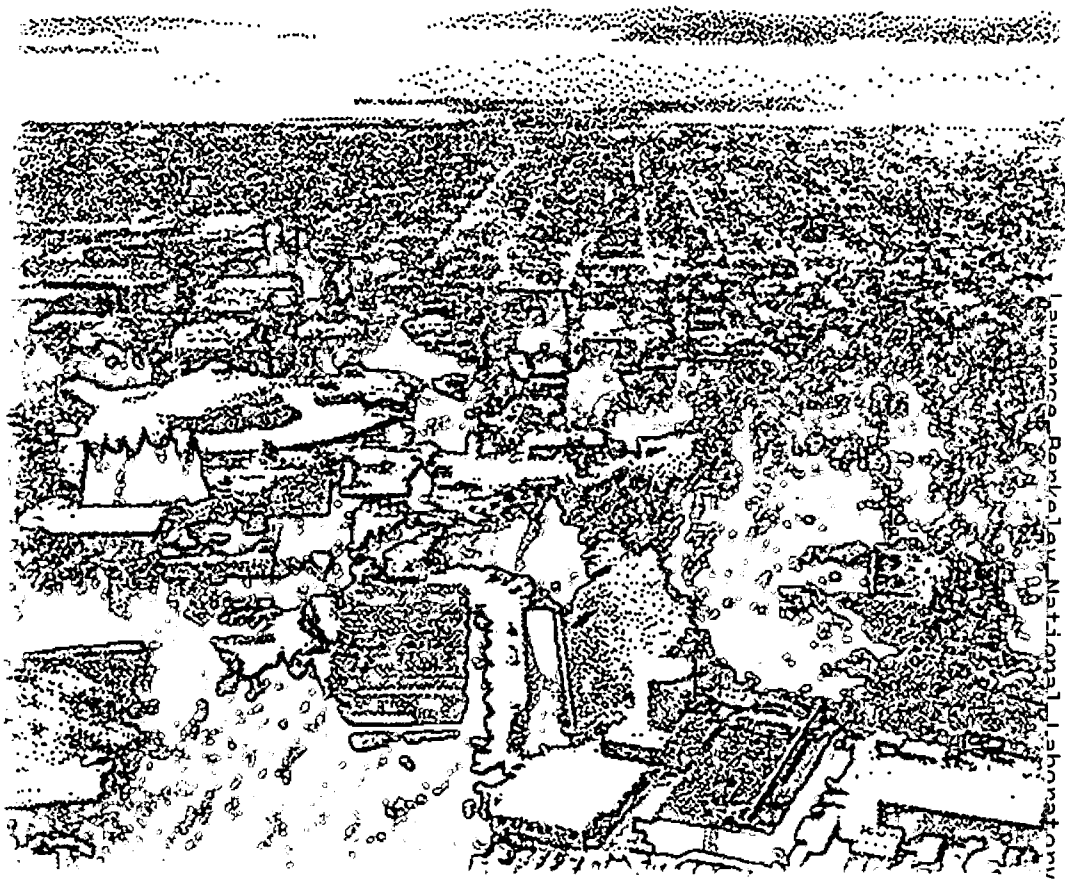

REFERENCE COPY
Does Not
Circulate

Annex

Copy 1

LBNL-47349

DISCLAIMER

This document was prepared as an account of work sponsored by the United States Government. While this document is believed to contain correct information, neither the United States Government nor any agency thereof, nor the Regents of the University of California, nor any of their employees, makes any warranty, express or implied, or assumes any legal responsibility for the accuracy, completeness, or usefulness of any information, apparatus, product, or process disclosed, or represents that its use would not infringe privately owned rights. Reference herein to any specific commercial product, process, or service by its trade name, trademark, manufacturer, or otherwise, does not necessarily constitute or imply its endorsement, recommendation, or favoring by the United States Government or any agency thereof, or the Regents of the University of California. The views and opinions of authors expressed herein do not necessarily state or reflect those of the United States Government or any agency thereof or the Regents of the University of California.

LBNL-47349

McMillan-Mayer Solution Thermodynamics for a Protein in a Mixed Solvent

R. A. Curtis, J. Newman, H. W. Blanch and J. M. Prausnitz
Department of Chemical Engineering
University of California
and
Chemical Sciences Division
Lawrence Berkeley National Laboratory
University of California
Berkeley, CA 94720, U.S.A.

January 2001

This work was supported by the Director, Office of Science, Office of Basic Energy Sciences, Chemical Sciences Division of the U.S. Department of Energy under Contract Number DE-AC03-76SF00098.

McMillan-Mayer Solution Thermodynamics for a Protein in a Mixed Solvent

R.A. Curtis, J. Newman, H.W. Blanch, and J.M. Prausnitz
Chemical Engineering Department, University of California, Berkeley and Chemical Sciences Division, Lawrence Berkeley National Laboratory, Berkeley, CA, 94720, Fax # (510)-643-1228

Abstract

McMillan-Mayer solution theory is used to calculate the thermodynamic properties of solute/solvent systems from the set of solvent-averaged interactions between solute particles. To match experimental data, the independent variables of the McMillan-Mayer framework (temperature, the set of solvent chemical potentials, and the set of solute concentrations) need to be converted to the Gibbs framework where the independent variables are temperature, pressure, and the set of concentrations for all components. Previous conversions have been restricted to systems with a single solvent and one or more solutes. However, in the analysis of light-scattering data, it is sometimes necessary to consider multiple solvents. Here, we present the thermodynamics of McMillan-Mayer solution theory for a single protein solute and a mixed solvent of aqueous salt; we show that protein-salt preferential-interaction parameters can be readily determined from data reduction within the McMillan-Mayer framework. We provide a sample calculation of a liquid-liquid phase separation for protein solutions, wherein we convert the phase diagram from the McMillan-Mayer framework to the Gibbs framework. For the coexistence curve of the McMillan-Mayer phase diagram, the salt molality of a hypothetical outside solution is held constant, whereas for the coexistence curve for the Gibbs phase diagram, the salt molality of the light phase is held constant. The difference between the curves is determined by the preferential-interaction parameter. The two curves are identical only in the limiting case where the preferential-interaction parameter is zero, the solvent can be considered as a pseudo-one-component solvent.

Introduction

Salt-induced protein precipitation and salt-induced protein crystallization are extensively used separation methods in biochemistry and biotechnology. Salt-induced protein precipitation is commonly used as a first step in the purification of proteins because of its selectivity and low cost, and salt-induced protein crystallization is often used for obtaining protein crystals for x-ray-diffraction studies. Optimizing these processes requires knowledge of the protein-aqueous-electrolyte phase diagrams as a function of the solution conditions, such as salt type, salt concentration, temperature, and pH. The thermodynamics of protein solutions depends crucially on the intermolecular interactions between proteins, salt ions, and water. Because these interactions are not

well understood, physically realistic simplifying assumptions are needed to determine the phase diagrams.

When there are large differences in the concentrations of the components in a solution, thermodynamic properties are commonly calculated from statistical-mechanical models where the inputs are solute-solute interactions averaged over positions of solvent molecules where the solutes are the dilute components and the solvents are the concentrated components. The averaging process reduces the order of the effective Hamiltonian such that calculations can be made assuming a pseudo one-component system. Models based on effective solute-solute interactions are in the framework of McMillan-Mayer solution theory where the n-body solvent-averaged effective interaction plays the same role as the n-body potential does in imperfect-gas theory [1]. Accordingly, the theories used to calculate thermodynamic properties of gases can be used to calculate the thermodynamic properties of liquid solutions where solute molecules interact through the solvent, provided that the n-body interaction energies are replaced with the n-body potentials of mean force.

For a single protein dissolved in an aqueous electrolyte solution, because typically the salt and water are each at a much greater concentration than the protein, we consider the salt and water as a mixed solvent; the protein is the solute. However, determining the effective protein-protein interactions from Boltzmann-averaging over positions of salt and water is beyond the scope of statistical mechanics. The advantage of using McMillan-Mayer theory is that the effective protein-protein interactions can be measured using a variety of techniques. Consequently, most theoretical work on protein-solution phase diagrams is based on a simplified form of the protein-protein-interaction potential function which is fit to experimental results from light scattering or osmometry [2-8].

Statistical mechanics provides a method for calculating a generating function from which all other equilibrium properties can be derived using standard thermodynamic calculations. However, the thermodynamic framework for calculating properties from the generating function must be chosen such that the independent

variables of the framework match those of the statistical-mechanical ensemble employed by the calculations. For McMillan-Mayer solution theory, the independent variables are the set of solvent chemical potentials, solute concentration, and temperature. However, most experimental properties are measured in the Gibbs framework where the independent variables are the set of molalities (other than that of the principal solvent), temperature, and pressure. Thus, the results of a theoretical model must be converted into the Gibbs (or Lewid-Randall) framework that uses conventional experimental variables.

Friedman [9] showed how the McMillan-Mayer framework can be converted to that of Gibbs for the primitive model of aqueous electrolyte solutions where the ions interact through water-mediated potentials of mean force. Friedman's work has been extended by Simonin [10], Haynes and Newman [11] and Zoeller et al. [12]; however in all previously studied systems there is only one solvent and one or more solutes. Inherent in these previous publications is the implicit restriction that the concentrations of the solutes are of similar magnitude and preferably low.

In some cases however, it is necessary to consider a ternary (or higher) mixture as a mixed-solvent system. For example, in reduction of light-scattering data for systems containing one high-molecular-weight component and two low-molecular-weight components, the latter two are considered as a mixed solvent. In interpreting light-scattering data for proteins in mixed solvents, the macromolecule-solvent preferential interaction is determined from comparing results from the pseudo-solvent framework with those from a mixed-solvent framework. As an example, Vrij and Overbeek [13] have studied charged colloidal particles in salt solutions using light scattering. They showed that the measured molecular weights need to be corrected by factors of 1.10 to 1.45 if the aqueous salt solution is considered as a pseudo-one-component instead of a mixed solvent. From the difference, the authors determined the amount of negative adsorption of salt on the colloidal particles.

Here, we describe a similar system containing one protein solute and a binary solvent of salt and water. While we present details for this specific ternary system, the results are readily generalized for any number of solutes dissolved in a multi-component solvent. Casassa and Eisenberg [14] have presented a thermodynamic analysis for a solute in a multi-component solvent for the Gibbs framework. Here, we show that protein-salt preferential interactions are directly determinable from data analyzed within the McMillan-Mayer framework. We then use results for the protein-salt preferential interaction to convert the independent variables of the McMillan-Mayer framework to those of a modified Gibbs framework where the independent variables are temperature, pressure, salt molality, and protein concentration. This conversion allows us to generate protein phase diagrams at constant pressure and constant salt molality, in contrast to the McMillan-Mayer framework where all phase diagrams are determined as functions of the less well-defined set of solvent chemical potentials.

The first section summarizes the essentials of McMillan-Mayer solution theory. The theory of preferential interactions is given in the following section within the McMillan-Mayer framework. In the final section, to illustrate our discussion, we calculate the liquid-liquid phase diagram for protein solutions in the modified Gibbs framework and compare it with that in the McMillan-Mayer framework.

Essentials of McMillan-Mayer Solution Theory

Consider the system shown in Figure (i) where a semi-permeable membrane separates an inside solution containing water (1), protein (2), and salt (3) and an outside solution that contains only solvent molecules, salt and water. The activities of the solvent molecules are the same for the inside and the outside solutions because they are permeable to the membrane. The thermodynamic properties of the outside solution are determined by three intensive properties chosen to be either the set of temperature, T, and chemical potentials of the solvent components, μ_1 and μ_3, or the set of temperature, outside-solution pressure, p_o, and outside-solution salt molality, $m_{3,o}$. In McMillan-Mayer solution theory, the properties of the inside solution are determined from the protein concentration, c_2, and the condition of osmotic equilibrium, which relates the

thermodynamics of the inside solution to that of the reference or outside solution. Thus the independent variables in the McMillan-Mayer framework are T, μ_1, μ_3, and c_2 or equivalently T, p_o, $m_{3,o}$, and c_2.

Thermodynamic properties of the inside solution are determined from the generating function that is the energy whose independent variables are T, μ_1, μ_3, and c_2, given by the McMillan-Mayer free energy, F. F is related to osmotic pressure, Π, and solute chemical potential, μ_2, by

$$F/V = -\Pi + \mu_2 c_2 \tag{1}$$

where V is the volume of the solution. The differential of F is

$$d(F/V) = \mu_2 dc_2 - (c_{1,i} - c_{1,o})d\mu_1 - (c_{3,i} - c_{3,o})d\mu_3 - (s_i - s_o)dT \tag{2}$$

Subscript o refers to the outside solution, introduced to distinguish properties of the outside solution from those of the inside solution, denoted by subscript i. c_j refers to molar concentration of component j and s refers to entropy per unit volume. From a model for the McMillan-Mayer free energy, all other thermodynamic properties of interest can be derived from the appropriate manipulations of Equations (1) and (2). For example, the protein chemical potential is given by the partial differential of Equation (2),

$$\mu_2 = \left(\frac{\partial F/V}{\partial c_2}\right)_{T,\mu_1,\mu_3} . \tag{3}$$

The pressure of the inside solution is given by the sum of the outside-solution pressure and the osmotic pressure where the osmotic pressure is calculated from Equations (1) and (3) as

$$\Pi = -F/V + \mu_2 c_2 . \tag{4}$$

An additional thermodynamic quantity of interest is the concentration of salt in the inside solution. This can be calculated from the a partial differential of Equation (2),

$$c_{3,i} = c_{3,o} - \left(\frac{\partial F/V}{\partial \mu_3}\right)_{T,\mu_1,c_2} . \tag{5}$$

Models for the McMillan-Mayer free energy F are based on statistical mechanics where there is a direct analogy between a system of gas molecules interacting through a vacuum and a system of solute particles interacting through a continuous solvent. The residual Hemlholtz energy, A^{res}, for a pure gas in terms of the set of n-body interaction potentials and gas density is the same function as the excess McMillan-Mayer energy function for a solute in a solvent in terms of the set of n-body potentials of mean force and the solute density. This mapping is symbolized by

$$A^{res}(c,T) \rightarrow F^{ex}(c_2,T,\mu_1,\mu_3) \tag{6}$$

where the left-hand side of Equation (6) refers to the pure gas and the right-hand side refers to the solute/mixed-solvent system. A residual property, denoted by superscript res, is the difference of the real-system property and that of an ideal gas at the same temperature and density. An excess property, denoted by ex, is the difference of the real-system property and the ideal property evaluated at the same temperature, solute concentration, and the set of solvent chemical potentials; an ideal solution is a solution where the solute molecules do not interact as discussed below. Because the solute/solvent system has two more degrees of freedom than those of the pure gas, the set of solvent chemical potentials need to be included as independent variables in the calculation of F^{ex}. These variables are contained in the description of the set of n-body potentials of mean force, $\{W^{(n)}\}$. The gradients of these potentials give the forces between n solute particles with fixed positions averaged over positions of all solvent molecules. Because the averaging process involves only the solvent molecules, the potential of mean force is determined by the state of the outside solution or the variables (T, μ_1, μ_3) or the variables $(T, p_o, m_{3,o})$.

Equation (6) provides the route for calculating the excess McMillan-Mayer free energy by using the same statistical mechanical theories that are used for calculating properties of pure gases. Generally, in theories for calculating the thermodynamics of pure gases, the n-body interaction potentials are approximated by the sum of the two-body interactions, referred to as pairwise additivity. The corresponding approximation in McMillan-Mayer theory is known as the superposition approximation. With this

approximation, the excess McMillan-Mayer free energy is a function of temperature, protein concentration, and the two-body potential of mean force.

The total McMillan-Mayer free energy is given by the sum of the ideal and excess contributions

$$F = F^{id} + F^{ex} \tag{7}$$

where an ideal solution is denoted by superscript id. In an ideal solution, because the solute molecules do not interact with each other, $W^{(2)}$ is equal to zero. The McMillan-Mayer free energy of an ideal solution is given by

$$F^{id}/V = c_2\mu_2^{\theta} + c_2RT(\ln c_2 - 1) \tag{8}$$

where μ_2^{θ} is the protein infinite-dilution standard state of the defined by

$$\mu_2^{\theta} = RT\ln\frac{\lambda_2^3}{q_2} + RT\ln\gamma_2^{\infty}. \tag{9}$$

Here, λ_2 is the thermal wavelength of the protein, q_2 is the internal partition function of the protein molecule, and γ_2^{∞} is the protein infinite-dilution activity coefficient. The first term on the right-hand side of Equation (9) is a function of only temperature, whereas the second term on the right-hand side of Equation (9) is a function of the thermodynamic state of the outside solution that is equal to the reversible work of turning on the intermolecular interactions between a protein and the surrounding solvent molecules.

Preferential-interaction Parameter

Experimental measurements are performed as a function of the independent variables in the Gibbs framework, given by temperature, pressure, and protein and salt concentration. Consequently, for a predictive model, calculated thermodynamic properties in the McMillan-Mayer framework must be converted to give properties in the Gibbs framework. To perform this conversion, the inside-solution properties need to be related to the outside-solution properties. For example, to relate the inside-solution pressure to the outside-solution pressure, we need to determine the osmotic pressure. Similarly, the difference of the inside-solution salt molality and the outside-solution salt molality needs to be calculated. As outlined below, this difference can be evaluated in

the McMillan-Mayer framework using Equation (5) and an appropriate form for the McMillan-Mayer free energy. However, before continuing with that analysis, we provide a brief review of evaluating this difference in salt molality using variables in the Gibbs framework [14,15].

Consider adding a single protein to the inside solution of the system described in Figure (i) with the outside solution much larger than the inside solution. In the limit of low protein concentrations, none of the protein molecules and the local layers of solvent perturbation will overlap. Thus, the same amount of salt will redistribute across the membrane for each protein molecule added and the difference in salt molalities across the membrane will be proportional to the protein molality. Since the outside solution has a large volume, the addition will be at constant chemical potential of the diffusible species. This addition can be represented mathematically as

$$\left.\frac{m_{3,i} - m_{3,o}}{m_2}\right|_{m_2 \to 0} = \left(\frac{\partial m_3}{\partial m_2}\right)^{\infty}_{T,\mu_1,\mu_3} . \tag{10}$$

Here the term on the left-hand side of Equation (10) is the infinite-dilution preferential-interaction parameter expressed in molality units. The superscript infinity indicates that the quantity is evaluated in the limit of infinite dilution of protein, corresponding to the properties of the outside solution. If the protein interacts preferably with the salt, there will be an excess of salt on the inside solution relative to the outside solution. If the protein interacts preferably with the water, there will be a deficiency of salt on the inside solution. Subsequently, it follows that the preferential-interaction parameter provides a measure of the protein-salt interaction relative to the protein-water interaction. The left-hand side of Equation (10) can be measured experimentally by any technique that detects differences in salt molalities between two solutions. Common techniques include densimetry and differential refractometry.

Cassassa and Eisenberg [14] derived the following relation for the infinite-dilution value of the preferential-interaction parameter in the Gibbs framework

$$\left(\frac{\partial m_3}{\partial m_2}\right)^{\infty}_{T,\mu_1,\mu_3} = -\frac{(\partial\mu_2/\partial m_3)^{\infty}_{T,p,m_2}}{(\partial\mu_3/\partial m_3)^{o}_{T,p}} + \frac{\bar{v}_3^o}{V_m^o(\partial\mu_3/\partial m_3)^{o}_{T,p}} \tag{11}$$

Quantities with overbars refer to partial molar quantities with respect to the component indicated by the subscript. Superscript o denotes that the property is evaluated at the conditions of the outside solution. Consequently, $(\partial\mu_3/\partial m_3)^{o}_{T,p}$ is the variation in salt chemical potential with salt molality evaluated at zero protein concentration; it can be determined from activity-coefficient data for the outside salt solution. V_m is the specific molal volume of the solution (L/kg water). Because $(\partial\mu_2/\partial m_3)^{\infty}_{T,p,m_2}$ is evaluated at infinite dilution of protein, protein-protein interactions are negligible and the derivative can be evaluated from the ideal protein chemical potential using Equations (4), (8), and (9)

$$\left(\frac{\partial\mu_2}{\partial m_3}\right)^{\infty}_{T,p,m_2} = \left(\frac{\partial\mu_2^{\theta}}{\partial m_{3,o}}\right)_{T,p_o} - \frac{RT}{V_m^o}\bar{v}_3^o \tag{12}$$

We evaluate the derivative in Equation (12) in terms of the McMillan-Mayer definition because the McMillan-Mayer standard state is related to the solvation free energy of the protein, which can be calculated from statistical mechanics [16]. Because the derivative of Equation (12) is evaluated at infinite dilution of protein, all the properties on the right side of this equation are evaluated at the properties of the outside solution. The extra term on the right side of Equation (12) appears because the derivative is evaluated at constant protein molality (moles protein/kg water) instead of in terms of protein concentration (moles protein/L). Substituting this result into Equation (11) gives

$$\left.\frac{m_{3,i} - m_{3,o}}{m_2}\right|_{m_2\to 0} = -\frac{(\partial\mu_2^{\theta}/\partial m_{3,o})_{T,p_o}}{(\partial\mu_3/\partial m_3)^{o}_{T,p}} \tag{13}$$

Consequently, the preferential-interaction parameter is related to the derivative of the solvation free energy (or the infinite-dilution activity coefficient) with respect to salt molality.

Equation (13) forms the basis for the salting-out studies of Arakawa and Timasheff [17]. In the absence of protein-protein interactions (i.e. in sparingly soluble

protein solutions), the preferential-interaction parameter is related to the dependence of the protein chemical potential on salt concentration. Arakawa and Timasheff [17] determined the infinite-dilution protein activity coefficient from measurements of the protein-salt preferential-interaction parameter. From the infinite-dilution activity coefficient, the authors correlated protein crystal solubility with the assumption that the protein crystal is a pure phase. Although the protein crystal contains a significant amount of solvent, the authors nevertheless obtained semi-qualitative agreement between protein solubility and the measured preferential-interaction parameters, stressing the importance of the relation between the protein solvation free energy and protein solubility.

The analysis above has been concerned with calculating the redistribution of salt in infinitely-dilute protein solutions where the redistribution results from the perturbation of salt molality in the domain of a single protein. In solutions of finite protein concentration, the regions of solvent perturbation overlap. Subsequently, the preferential-interaction parameter is not necessarily linear in protein molality, because the number of ions involved in the interactions of two or more domains of solvent perturbation is not necessarily equal to their sum. To account for these effects, it is easier to evaluate the preferential-interaction parameter in the McMillan-Mayer framework, where the independent variables match those of the preferential-interaction parameter (i.e. μ_1 and μ_3).

Consider expanding the difference in salt concentration, $c_{3,i} - c_{3,o}$, in a power series in protein concentration

$$c_{3,i} - c_{3,o} = \sum_{n>1} \Delta c_{3,n} c_2^n \tag{14}$$

Here, the nth-order coefficients, $\Delta c_{3,n}$ are related to the salt deficiency or excess of the nth-order interaction between solvent layers. Thus, the first-order coefficient is related to the amount of salt perturbation due to a single protein. The second-order coefficient is related to the amount of excess or deficiency of salt in the two-body interaction minus that of two non-overlapping solvent layers. The preferential-interaction parameter expressed in units of molar volume concentration is obtained by dividing Equation (14)

by protein concentration. The thermodynamic calculations in the McMillan-Mayer framework use concentration units because volume is the independent extensive variable in this framework.

To determine the coefficients of Equation (14), we use Equation (5) along with the osmotic virial expansion for the McMillan-Mayer free energy, given by

$$\frac{F}{VRT} = c_2 \frac{\mu_2^\theta}{RT} + c_2\left[\ln c_2 - 1\right] + c_2^2 B_{22} + c_2^3 B_{222} + .. \tag{15a}$$

where B_{22} is the second virial coefficient, B_{222} is the third virial coefficient, etc. The nth virial coefficient is related to a volume integral of the n-body potential of mean force.

Substituting Equation (15a) into Equation (5) gives the desired expansion in protein concentration for the difference in salt concentration. The first-order coefficient is related to the derivative of the standard-state potential with respect to salt chemical potential, whereas the nth-order coefficients are related to derivatives of the n-body pmfs with respect to salt chemical potential. Because functions of the properties of the outside solution are usually known in terms of (T, p_o, $m_{3,o}$) instead of (T, μ_1, μ_3), the variables need to be changed according to

$$\left(\frac{\partial F/V}{\partial \mu_3}\right)_{T,\mu_1,c_2} = \left(\frac{\partial F/V}{\partial m_{3,o}}\right)_{T,p_o,c_2}\left(\frac{\partial m_{3,o}}{\partial \mu_3}\right)_{T,\mu_1} + \left(\frac{\partial F/V}{\partial p_o}\right)_{T,m_{3,o},c_2}\left(\frac{\partial p_o}{\partial \mu_3}\right)_{T,\mu_1} \tag{15b}$$

After the change of variables, the infinite-dilution value of the preferential-interaction parameter in concentration units is given by

$$\left.\frac{c_{3,i} - c_{3,o}}{c_2}\right|_{c_2 \to 0} = \Delta c_{3,1} = -\left(\frac{\partial \mu_2^\theta}{\partial m_{3,o}}\right)_{T,p_o} \frac{1 - \bar{v}_3^o c_{3,o}}{\left(\partial \mu_3 / \partial m_3\right)_{T,p}^o} - \bar{v}_2^\infty c_{3,o} \tag{16}$$

Algebraic rearrangement shows that Equation (16) is identical to Equation (13).

The second-order coefficient is given by

$$\Delta c_{3,22} = -\frac{\left(1 - \bar{v}_3^o c_{3,o}\right) RT}{\left(\partial \mu_3 / \partial m_3\right)_{T,p}^o}\left(\frac{\partial B_{22}}{\partial m_{3,o}}\right)_{T,p_o} - c_{3,o} RT \left(\frac{\partial B_{22}}{\partial p_o}\right)_{T,m_{3,o}} \tag{17}$$

Here, the sign of the first term on the right of Equation (17) is given by the sign of $\left(\partial B_{22}/\partial m_{3,o}\right)_{T,p_o}$. This relation has interesting physical implications. For solutions of proteins in dilute aqueous electrolytes, B_{22} decreases as the salt concentration is raised because the electric double-layer repulsion between charged proteins decreases with rising ionic strength. Based on Equation (17), this trend implies that the amount of salt contained in overlapping double layers minus that in two non-overlapping double layers is greater than zero. This result is consistent with DLVO theory, where the electrostatic repulsion is related to an imbalance in osmotic pressure due to a concentration of salt between protein molecules higher than that away from the protein molecules.

In another relation between the osmotic virial equation of state and the preferential-interaction parameter, consider the system shown in Figure (ii). Here, the polymer is one of the solvent components. Asakura and Oosawa [18] showed that an effective two-body attraction between protein molecules results from averaging over positions of polymer molecules. The attraction results from the hard-sphere interactions of the polymer molecules that excludes polymer from the space between two proteins in close proximity. If the surface-to-surface separation of two protein molecules is less than the effective hard-sphere diameter of the polymer, the polymer is squeezed out from between the protein surfaces and the osmotic pressure between the proteins is less than that outside, resulting in an effective attraction. As the polymer concentration rises, the imbalance in osmotic pressure is greater and the effective attraction increases. According to Equation (17), this trend implies that the concentration of polymer molecules that experience the two-body interaction minus that of two infinitely dilute protein molecules is greater than zero. The physical basis for this phenomenon is illustrated in Figure (ii) where the zone of polymer exclusion is reduced when the polymer molecules are squeezed out from between the protein molecules.

To illustrate the previous paragraphs, we calculate the preferential interaction between lysozyme and sodium chloride up to second order in protein concentration using Equations (16) and (17). The first-order term is related to the solvation free energy of the

protein molecule. In concentrated salt solutions, the solvation free energy of protein molecules has been correlated with the following relation [19]:

$$\left(\frac{\partial \mu_2^{\theta}}{\partial m_3}\right)_{P_o} \sim -\Lambda_2 + \left(\frac{d\sigma}{dm_3}\right) S_2 . \tag{18}$$

The first term on the right-hand side of Equation (18) is the contribution from favorable electrostatic interactions between the charge on the protein surface and salt ions. For salt molalities greater than 0.5 molal, this term is proportional to the dipole moment of the protein, Λ_2. The second term is related to the work to form a cavity in the salt solution. The incremental free energy is proportional to the molal surface-tension increment of the salt, ($d\sigma/dm_3$), multiplied by the surface area of the protein molecule, S_2. Because all salts have positive surface-tension increments, this effect always leads to the preferential exclusion of salt in the domain of the protein.

In the calculation of the preferential-interaction parameter, the second-order term is also included in the calculation using the first term on the right of Equation (17). The derivative of B_{22} with respect to salt molality has been evaluated numerically from B_{22} data for lysozyme in solutions of sodium chloride [20]. All other properties are shown in Table (i).

In Figure (iii), the inside-solution salt molality, calculated with and without the second-order correction term, is plotted versus protein concentration for an outside solution salt molality of 1.0. For all protein concentrations, the salt is excluded from the inside solution. This is typical of most salt solutions at molalities greater than 0.5 where salting-out behavior is observed. Generally, the unfavorable surface tension-increment effect is greater than the favorable electrostatic interaction between the protein dipole and the ion atmosphere. This results in an increase in the infinite-dilution activity coefficient and a reduction in protein solubility. The second-order correction is not significant at protein concentrations less than 100 g/L; at higher protein concentrations the preferential exclusion of the salt decreases because the pmf is more attractive with the addition of salt. However, at protein concentrations greater than 100 g/L, it is likely that higher-

order interactions are significant. Consequently, truncating the virial expansion at second order may introduce significant error.

The inset of Figure (iii) shows that the preferential-interaction parameter is proportional to the outside-solution salt molality for a protein molality of 0.005 molal (~65 g/L). This proportionality is a consequence of the law of mass action.

Phase-Equilibrium Calculations

McMillan-Mayer Phase Equilibrium

Consider the case of determining the liquid-liquid equilibrium for the system of protein dissolved in an aqueous electrolyte solution (the liquid-liquid equilibrium for solute in a solvent is analogous to the liquid-vapor equilibrium of a pure substance). The light liquid phase (l) and the dense liquid phase (d) have the same outside solution due to the equilibrium condition that each solvent species has the same chemical potential in all phases. The choices of the independent variables are made from the set of thermodynamic variables corresponding to the framework. The natural intensive thermodynamic variables in the McMillan-Mayer framework for the two-phase system are T, c_2^l, c_2^d, p_o, and $m_{3,o}$. According to the phase rule, there are three intensive degrees of freedom. Here, the properties of the outside solution, T, p_o, and $m_{3,o}$ are the independent variables; c_2^l and c_2^d are calculated from the two equilibrium conditions

$$p_o + \Pi^l = p_o + \Pi^d \tag{19}$$

and

$$\mu_2^l = \mu_2^d. \tag{20}$$

Because both phases have the same outside solutions, the outside-solution pressure cancels in Equation (19) that becomes

$$\Pi^l = \Pi^d. \tag{21}$$

The osmotic pressure and protein chemical potential are determined from a model whose inputs are the two-body potential of mean force, the protein concentration, and temperature. The potential of mean force is the same for both phases because it is a function of the outside-solution variables, T, p_o, and $m_{3,o}$.

On a coexistence curve, one of the independent variables varies and the other independent variables are constant. In this illustration, we generate cloud-point (temperature) curves where coexistence temperature is plotted versus the light and dense-phase protein concentrations. In the McMillan-Mayer framework, the outside-solution pressure and the outside-solution salt molality are constant, whereas the pressure and the salt molality of the equilibrated phases vary along the cloud-point curve. The pressure is given by the sum of the outside-solution pressure and the osmotic pressure and the salt molality is determined from the preferential-interaction parameter that can be calculated from Equations (14), (16), and (17).

When salt and water are considered as a pseudo-solvent, it is implicitly (and erroneously) assumed that the preferential-interaction parameter expressed in molality units is zero, i.e. the outside-solution salt molality is equal to the inside-solution salt molality. Because the preferential-interaction-parameter analysis is not used in the determination of the cloud-point curve, this curve is independent of the treatment of the solvent as long as we choose the outside-solution salt molality of the mixed-solvent system equal to that of the pseudo-solvent. However, the pseudo-solvent condition gives the incorrect result that the salt molality in the light phase is equal to that in the dense phase.

Phase Equilibrium in the Gibbs Framework

Cloud-point temperature curves are generated by cooling protein solutions at constant pressure until the onset of phase separation as observed by a discontinuous change in the turbidity of the solution. Because only a differential amount of the dense phase is formed, the salt molality in the light phase is given by the salt molality of the protein solution before phase separation. Thus to match experimental data, it is desirable to generate coexistence curves at constant pressure and at constant salt molality of the light phase instead of generating curves at constant properties of the hypothetical outside solution. To perform calculations in this experimental framework, we first use McMillan-Mayer solution theory to determine the thermodynamic properties from the two-body potential of mean force. Because the potential of mean force is a function of

the properties of the hypothetical outside solution, T, p_o, and $m_{3,o}$, we than need to relate the variables of the McMillan-Mayer framework to those of the modified Gibbs framework. The properties of the outside solution also determine the protein infinite-dilution standard state and the chemical potentials of the solvent components that are also required for calculation of phase equilibria in the Gibbs framework.

We need the outside pressure, p_o, and the outside-solution salt molality, $m_{3,o}$, as a function of T, p_i, c_2, $m_{3,i}$. The preferential-interaction parameter relates the difference in salt concentration of the inside and of the outside solution to the McMillan-Mayer free energy,

$$c_{3,i} - c_{3,o} = -\left(\frac{\partial F/V}{\partial \mu_3}\right)_{T,\mu_1,c_2} \sim \Im\left[c_2, T, W^{(2)}\left(T, p_o, m_{3,o}\right), \mu_2^{\theta}\left(T, p_o, m_{3,o}\right)\right] \quad (22)$$

where $\Im$ denotes a function of those variables contained in the brackets and where the salt concentrations are given by

$$c_{3,o} = \frac{m_{3,o}}{V_{m,o}\left(T, p_o, m_{3,o}\right)} \quad (23)$$

and

$$c_{3,i} = \frac{m_{3,i}}{V_{m,i}\left(T, p_i, c_2, m_{3,i}\right)}. \quad (24)$$

The outside-solution pressure can be determined from the osmotic pressure given the pressure of the inside solution

$$p_o = p_i - \Pi \quad (25)$$

where

$$\Pi \sim \Im\left[c_2, T, W^{(2)}\left(T, p_o, m_{3,o}\right)\right] \quad (26)$$

Relations given by Equations (22) and (26) provide two implicit relations in $m_{3,o}$ and p_o which can be obtained in terms of the independent variables of the inside solution, T, p_i, c_2, and $m_{3,i}$.

In this phase equilibrium there are three degrees of freedom. The temperature, pressure, and salt molality of the light phase, $m_{3,i}^{l}$, are a convenient set of independent

variables. The salt molality in the dense phase, $m_{3,i}^{d}$ and the protein concentrations in the light and dense phases, c_2^{l} and c_2^{d} are then determined from the equilibrium relations

$$\mu_1^{l} = \mu_1^{d} \tag{27}$$

$$\mu_2^{l} = \mu_2^{d} \tag{28}$$

$$\mu_3^{l} = \mu_3^{d} \tag{29}$$

Because the chemical potentials of the solvent components in the light phase are equal to those in the dense phase, these phases have the same outside solution. Thus, we can replace these equilibrium criteria (Equations 27 and 29) with the following:

$$m_{3,o}^{l} = m_{3,o}^{d} \tag{30}$$

and

$$p_o^{l} = p_o^{d} \tag{31}$$

Equations (30) and (31) provide a more direct method for equating the chemical potentials of the salt and of the water avoiding the additional calculation of the salt and water chemical potentials. Because both phases are also at the same pressure, Equation (31) is also satisfied by

$$\Pi^{l} = \Pi^{d}. \tag{32}$$

In the Gibbs framework, the salt molality of the light phase and the pressure remain constant along the cloud-point curve and the properties of the outside solution vary as a function of temperature.

For the pseudo-one-component-solvent case in the Gibbs framework, because the salt molality of the light phase is equal to that in the dense phase, the phase-equilibrium criteria reduce to Equations (28) and (32), which need to be solved for the light and dense-phase protein concentrations. These conditions are identical to the McMillan-Mayer equilibrium conditions. The difference in the two systems of equations is that the outside-solution pressure varies along a Gibbs cloud-point curve, in contrast to the McMillan-Mayer cloud-point curve, where the outside-solution pressure is held constant. The difference in the outside-solution pressure of the Gibbs framework and that of the

McMillan-Mayer is given by the osmotic pressure of the solution that is on the order of 0.01 atmospheres for typical protein solutions. Because it is unlikely that the potential of mean force changes significantly over this range, we expect that the cloud-point curve in the Gibbs framework is similar to that of McMillan-Mayer for the case of a single-component pseudo-solvent and consequently also similar to the McMillan-Mayer cloud-point curve for the case of a mixed-solvent at the same outside-solution salt molality as the pseudo-solvent.

If the protein-salt preferential interaction is strong, there will be a large difference in the salt molality of the dense phase and that of the light phase. In this case, the salt is treated as a separate component and we need the additional phase equilibrium criterion of Equation (30) to solve for the salt molality in the dense phase given that in the light phase. In the modified Gibbs framework, we can generate a phase diagram at constant pressure and salt molality of the light phase. Here the outside-solution salt molality and the outside-solution pressure vary along the cloud-point curve in contrast to the McMillan-Mayer curve where the outside-solution properties are held constant. As mentioned in the preceding paragraph, we do not expect the small changes in outside-solution pressure to alter the shape of the cloud-point curve. In this study, we determine the effect of varying the outside-solution salt molality along the Gibbs cloud-point curve versus holding this variable constant along that of the McMillan-Mayer framework.

To simplify the computation, we ignore the dependence of the potential of mean force and the protein infinite-dilution standard state on the outside-solution pressure. Because osmotic pressures of protein solutions are on the order of 0.01 atm, we expect that the potential of mean force and the protein infinite-dilution standard state can be approximated by their values evaluated at the pressure of the inside solution, set to 1.0 atm.

Phase-Equilibrium Results

To illustrate our discussion, we fit the liquid-liquid equilibrium data for lysozyme in sodium-chloride solutions using the McMillan-Mayer and the Gibbs frameworks. We

use a simple statistical-mechanics model [21-22] to calculate the thermodynamic properties of the McMillan-Mayer phases. Here, the protein-protein interaction in the light and dense fluid phases is given by the same two-body potential of mean force. This two-body pmf is given by a hard-sphere term and a power-law attractive interaction:

$$W^{(2)}(r) = \begin{cases} \infty & \text{for } r \le d_2 \\ -\varepsilon\left(\dfrac{r}{d_2}\right)^{-n} & \text{for } r > d_2 \end{cases} \tag{33}$$

where d_2 is the hard-sphere protein diameter, r is center-to-center separation, n is the power-law exponent and ε is the interaction strength at contact. The random-phase approximation is used to calculate the thermodynamic properties from the power-law potential. The RPA is a first-order perturbation theory for the McMillan-Mayer free energy (or the analogous Helmholtz energy for a pure gas). The reference system is a fluid of hard spheres and the attractive power-law potential gives the perturbation. The McMillan-Mayer free energy is given by

$$\frac{F}{V} = c_2\mu_2^0 + c_2RT[\ln c_2 - 1] + RT\frac{4\eta - 3\eta^2}{(1-\eta)^2} + \frac{1}{2}N_{av}^2 c_2^2 \int_{d_2}^{\infty} 4\pi r^2 W_{pert}^{(2)}(r)\,dr \tag{34}$$

where η is the hard-sphere packing fraction ($=\pi d_2^3\rho_2/6$), ρ_2 is protein number density, R is the gas constant, N_{av} is Avogadro's number, and $W_{pert}^{(2)}$ refers to the attractive power-law contribution to $W^{(2)}$. The first two terms on the right side of Equation (34) give the ideal contribution to the McMillan-Mayer free energy. The contribution of the hard-sphere reference system is calculated from the Carnahan-Starling equation of state [23], given by the third term on the right-hand side of Equation (34). The last term includes the contribution of the attractive power-law potential to the McMillan-Mayer free energy.

The protein chemical potential is obtained from substituting Equation (34) into Equation (3). Similarly, the osmotic pressure is obtained from the protein chemical potential using Equation (4). After substituting in the attractive power-law potential, we have the following expressions

$$\mu_2 = \mu_2^0 + RT\ln c_2 + RT\frac{8\eta - 9\eta^2 + 3\eta^3}{(1-\eta)^3} - 2\pi R c_2 N_{av}\frac{d_2^3}{n-3}\frac{\varepsilon}{k_B} \tag{35}$$

and

$$\frac{\Pi}{c_2RT}=\frac{1+\eta+\eta^2-\eta^3}{(1-\eta)^3}-2\pi c_2N_{av}\frac{d_2^3}{n-3}\frac{\varepsilon}{k_BT}. \tag{36}$$

where we use Equation (9) for μ_2^θ and k_B is Boltzmann's constant. The infinite-dilution activity coefficient is determined from the solvation free energy of the protein. Here the protein solvation free energy is given by the integrated form of Equation (18), where the lower limit of integration gives the solvation free energy of the protein in salt-free water. This term cancels out in the phase-equilibrium calculations given here.

The interaction strength, ε is taken from Fornaseiro et al. [22] for fitting the phase-equilibrium data for lysozyme in solutions of sodium chloride where the salt molality ranges from 0.8 to 1.3 molal [24],

$$\varepsilon/k_B=750+120m_{3,o} \tag{37}$$

with n equal to 6. The calculated cloud-point curves are shown in Figure (iv) along with the experimental data for lysozyme in solutions of 7 % w/v (~1.3 molal) NaCl [24]. The dashed line refers to the McMillan-Mayer cloud-point curve; the outside-solution salt molality is held constant at 1.0 molal on this curve. The solid line refers to the Gibbs cloud-point curve; the salt molality in the light phase is set to 1.0 molal on this curve.

The main purpose of this work is to contrast the cloud-point curves generated in the McMillan-Mayer framework and those generated in the Gibbs framework. To simplify the calculation, we have used a simplified form of the two-body potential of mean force and a statistical mechanical model that neglects higher-body interactions. For this reason, the model does not describe the experimental data accurately; however, more sophisticated (and more realistic) statistical-mechanical models can be used to achieve better agreement with the data.

The salt molality in the light and dense phases at coexistence depends on the outside-solution salt molality which is different for the coexistence calculation in the

Gibbs framework and for that in the McMillan-Mayer framework. This is demonstrated by Figure (v) that shows the coexistence temperature versus inside and outside-solution salt molality. Because the salt is excluded in the domain of the protein, the outside solution is always at a higher salt molality than that of the light and dense phases. In the calculation performed in the Gibbs framework, the light-phase salt molality is constant. Thus the outside-solution salt molality increases with rising light-phase protein concentration (or rising temperature) because the amount of preferential exclusion of salt is proportional to protein concentration. This is in contrast to the McMillan-Mayer framework where the outside-solution salt molality is constant.

At a given coexistence temperature, calculation of the protein concentration in the light phase and that in the dense phase is independent of the framework. The difference is that the cloud-point curves are evaluated at different properties of the outside solution. Because the effect of pressure is negligible, we are only concerned with the dependence of the phase diagram on the outside-solution salt molality. The length of the tie line joining the light and dense-phase protein concentrations increases with rising protein-protein attraction. Here, at a given temperature, the light and dense-phase protein concentrations of the Gibbs cloud-point curve are evaluated at a higher outside-solution salt molality than those for the McMillan-Mayer cloud-point curve. Because the protein-protein attraction is proportional to the outside-solution salt molality, the phase diagram is wider in the Gibbs framework relative to the McMillan-Mayer framework. The largest difference between the two cloud-point curves occurs near the critical point where the outside-solution salt molality of the Gibbs cloud-point curve is a maximum.

Figure (vi) compares the cloud-point curves generated for a set of different salt molalities. As salt molality rises from 1.0 to 2.0 molal, the protein-protein attraction is enhanced and the solutions become less stable giving precipitation at higher temperatures. Here, the dashed lines refer to the McMillan-Mayer cloud-point curves evaluated at a constant outside-solution salt molality equal to the salt molality of the light phase on the Gibbs cloud-point curves denoted by the solid lines. Because of this equality, the difference in the outside-solution salt molalities of each set of curves is

given by the preferential exclusion of the salt from the light-phase of the Gibbs cloud-point curve. The amount of preferential exclusion of salt from the light phase is proportional to the preferential-interaction parameter multiplied by the protein concentration of the light phase. As shown in the inset of Figure (iii), the preferential-interaction parameter is also proportional to the salt molality of the solution at a given protein concentration. Consequently, as salt molality rises from 1.0 to 2.0 molal, the difference in the corresponding cloud-point curves is also magnified, as shown in Figure (vii) where the outside-solution salt molality minus light-phase salt molality is plotted versus light-phase protein concentration for the Gibbs phase diagram.

Conclusions

In the calculation of cloud-point curves, it is usually assumed that the aqueous salt solution can be considered to be a pseudo-one-component solvent; in that case, the salt molality of the light phase is identical to the salt molality of the hypothetical outside solution that determines the potential of mean force. We have shown that the error introduced by this approximation is determined by the magnitude of the preferential-interaction parameter. The preferential-interaction parameter is largest for conditions favorable for the salting-out of proteins: concentrated salt solutions and solutions of kosmotropic salts and for solutions of concentrated protein. As a result, the error introduced by the pseudo-solvent approximation increases as the critical point is approached from lower temperatures and also increases with rising salt molality. A similar correction factor is important in the determination of molecular weights of macromolecules from light-scattering data.

Nomenclature

A	Helmholtz energy
B_{22}	protein osmotic second virial coefficient
B_{222}	protein osmotic third virial coefficient
c	molar concentration
d	hard-sphere diameter
F	McMillan-Mayer free energy
k_B	Boltzmann's constant, = 1.38×10^{-23} J/K
m	molality
n	power-law exponent
N_{av}	Avogadro's number
p	pressure
q	intra-molecular partition
r	center-to-center separation
R	gas constant
s	entropy per unit volume
S	entropy
T	temperature
U	internal energy
$\bar{v}$	partial molar volume
V	volume
V_m	molal volume
$W^{(n)}$	n-body potential of mean force

<u>Greek symbols</u>

β	dimensionless inverse temperature
γ_i	activity coefficient of component i
γ_2^∞	protein infinite-dilution activity coefficient
ε	energy parameter
η	protein packing fraction

λ	thermal wavelength
Λ	dipole moment
μ	chemical potential
Π	osmotic pressure
ρ	number density
σ	surface tension

Subscripts

o	outside solution property
i	inside solution property
1	water
2	protein
3	salt

Superscripts

l	light-phase property
d	dense-phase property

Acknowledgements

For financial support, the authors are grateful to the Office for Basic Energy Sciences of the U.S. Department of Energy and to the National Science Foundation (Grant #CTS-9530793). Robin Curtis thanks Leo Lue for clarifying the statistical mechanics of McMillan-Mayer solution theory.

References

[1] W.G. McMillan, J.E. Mayer, J. Chem. Phys. 13 (1945) 276.

[2] N. Asherie, A. Lomakin, G.B. Benedek, Phys. Rev. Lett. 77 (1996) 4832.

[3] C. Haas, J. Drenth, W.W. Wilson, J. Phys. Chem. B 103 (1999) 2808.

[4] D. Rosenbaum, P.C. Zamora, C.F. Zukoski, Phys. Rev. Lett. 76 (1996) 150.

[5] Y. Chiew, D. Kuehner, H. Blanch, J. Prausnitz, AIChE J. 41 (1995) 2150.

[6] M. Malfois, F. Bonnete, L. Belloni, A. Tardieu, J. Chem. Phys. 105 (1996) 3290.

[7] R. Piazza, J. Cryst. Growth 196 (1999) 415.

[8] W. C. K. Poon, Phys. Rev. E 55 (1997) 3762.

[9] H.L. Friedman, J. Sol. Chem. 1 (1972) 387.

[10] J. Simonin, J. Chem. Soc. Faraday Trans. 96 (1996) 3510.

[11] C.A. Haynes, J. Newman, Fluid Phase Equil. 145 (1998) 255.

[12] N. Zoeller, L. Lue, D. Blankschtein, Langmuir 13 (1997) 5258.

[13] A. Vrij, J. T. G. Overbeek, J. Colloid Sci. 17 (1962) 570.

[14] E.F. Casassa, H. Eisenberg, Adv. Prot. Chem. 19 (1964) 287.

[15] C.F. Anderson, M.T. Record, J. Phys. Chem. 97 (1993) 7116.

[16] H. Wang, A. Ben-Naim, J. Phys. Chem. B 101 (1999) 1077.

[17] T. Arakawa, S.N. Timasheff, Meth. Enzymology 114 (1985) 49.

[18] S. Asakura, F. Oosawa, J. Polymer Sci. 33 (1958) 183.

[19] W. Melander, C. Horvath, Arch. Biochem.Biophys.183 (1977) 200.

[20] R.A.Curtis, A. Montaser, J.M. Prausnitz, H.W. Blanch, Biotech. Bioeng. 57 (1998) 11.

[21] A. Daanoun, C.F. Tejero, M. Baus, Phys. Rev. E 50 (1994) 2913.

[22] F. Fornaseiro, J. Ulrich, J.M. Prausnitz, Chem. Eng. Proc. 38 (1999) 463.

[23] N. Carnahan, K. Starling, J. Chem. Phys. 51 (1970) 635.

[24] M. Muschol, F. Rosenberger, J. Chem. Phys. 103 (1995) 10424.

[25] K.S. Pitzer, J.C. Peiper, R.H. Busey, J. Phys. Chem. Ref. Data 13 (1984) 1.

[26] K.S. Pitzer, Activity coefficients in electrolyte solutions. CRC press, Boca Raton (1991).

[27] Z.-B. Li, Y.-G. Li, J.-F. Lu, Ind. Eng. Chem. Res. 38 (1999) 1133.

Property	Reference
partial molar volumes	[25]
activity coefficient and osmotic coefficient	[26]
surface tension	[27]

Table i: Thermodynamic properties required to calculate preferential-interaction parameter. All properties refer to aqueous solutions of sodium chloride calculated as a function of salt molality and temperature.

List of Figures

Figure i: McMillan-Mayer solution theory describes the properties of the inside solution in terms of an outside solution that is at the same temperature and chemical potential of solvent components (salt and water) denoted by μ_1 and μ_3. Here, p is pressure, T is temperature, m_3 is salt molality, and Π is osmotic pressure. Subscripts o and i refer to outside and inside solutions, respectively. Quantities, $m_{3,i}$, Π, and μ_2 are determined from a model whose inputs are protein concentration, c_2, and the properties of the outside solution, either (μ_1, μ_3, T) or (p_o, $m_{3,o}$, T).

Figure ii: As shown in the inset, there is an effective two-body attraction between proteins immersed in a solution of polymers because polymer molecules are excluded from the region surrounding the protein causing an imbalance in the osmotic pressure of the polymer molecules. According to Equation (3.17), this implies that the number of polymer molecules per protein molecule is larger in solutions of concentrated proteins. Physically, the zones of exclusion overlap in concentrated protein solutions and the average polymer molality per protein molecule is higher in concentrated protein solutions than in dilute protein solutions where the exclusion regions do not overlap.

Figure iii: Plot of the inside-solution salt molality versus protein concentration for a hypothetical outside-solution salt molality of 1.0 molal. The dashed line refers to the calculation to first-order in protein concentration and the solid line refers to the calculation to second-order in protein concentration. In the inset, the preferential interaction parameter is plotted versus salt molality for a protein molality of 0.005 molal.

Figure iv: Cloud-point temperature curves correlated using the Gibbs framework or the McMillan-Mayer framework with the Random Phase Approximation and an attractive power-law potential. In the McMillan-Mayer cloud-point curve, the outside-solution salt molality is held constant at 1.0 molal, whereas the salt molality of the light phase is held constant at 1.0 molal in the Gibbs cloud-point curve. The experimental data for lysozyme in 7% w/v NaCl solution are from Muschol and Rosenberger (1997).

Figure v: Calculations of the coexistence temperature versus inside-solution or outside-solution salt molality for the Gibbs framework and for the McMillan-Mayer framework.

Figure vi: Cloud-point curves from the Gibbs framework and from the McMillan-Mayer framework for three salt molalities. The light-phase salt molality is constant along the Gibbs cloud-point curve, whereas the outside-solution salt molality is constant along the McMillan-Mayer cloud-pointcurve. The McMillan-Mayer cloud-point curves are similar to the Gibbs cloud-point curves for a one-component pseudo-solvent.

Figure vii: Difference in the outside-solution salt molality and that of the light phase for the Gibbs phase diagrams in Figure 3.8 where the symbols correspond to (■) 1.0 molal (▲) 1.5 molal and (●) 2.0 molal.

"Outside"	"Inside"
1 - water 3 - salt μ_1, μ_3, T $m_{3,o}$ p_o	1 - water 2 - protein 3 - salt μ_1, μ_3, c_2, T $\mu_2, m_{3,i}$ $p_i = p_o + \Pi$

Figure i

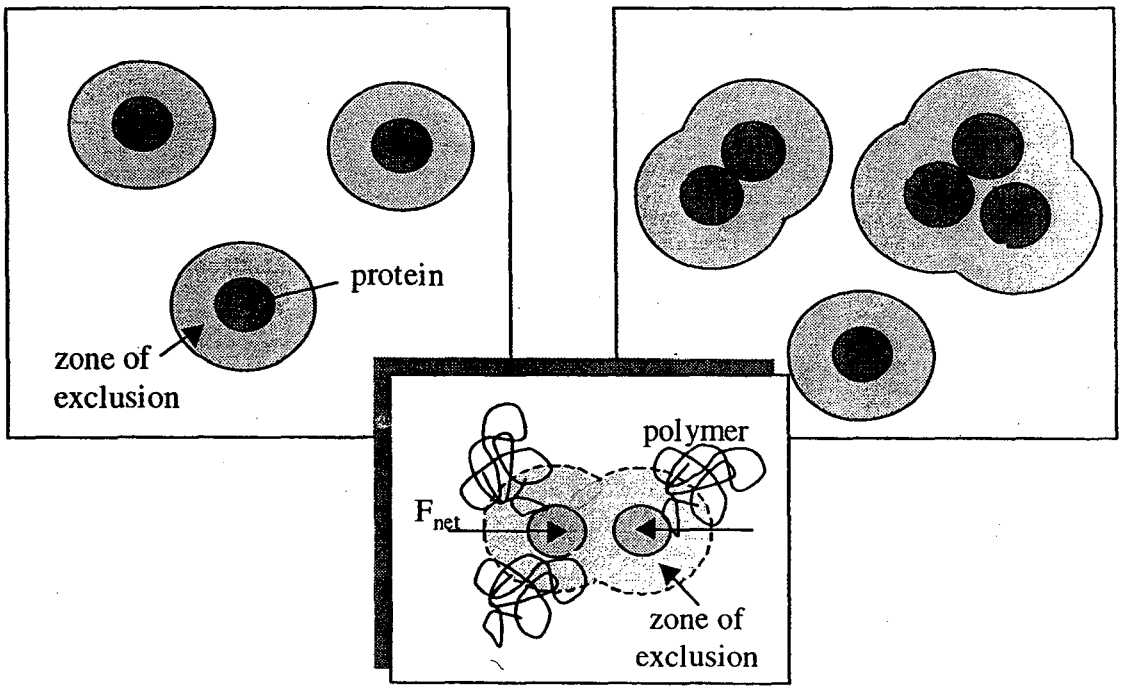

Figure ii

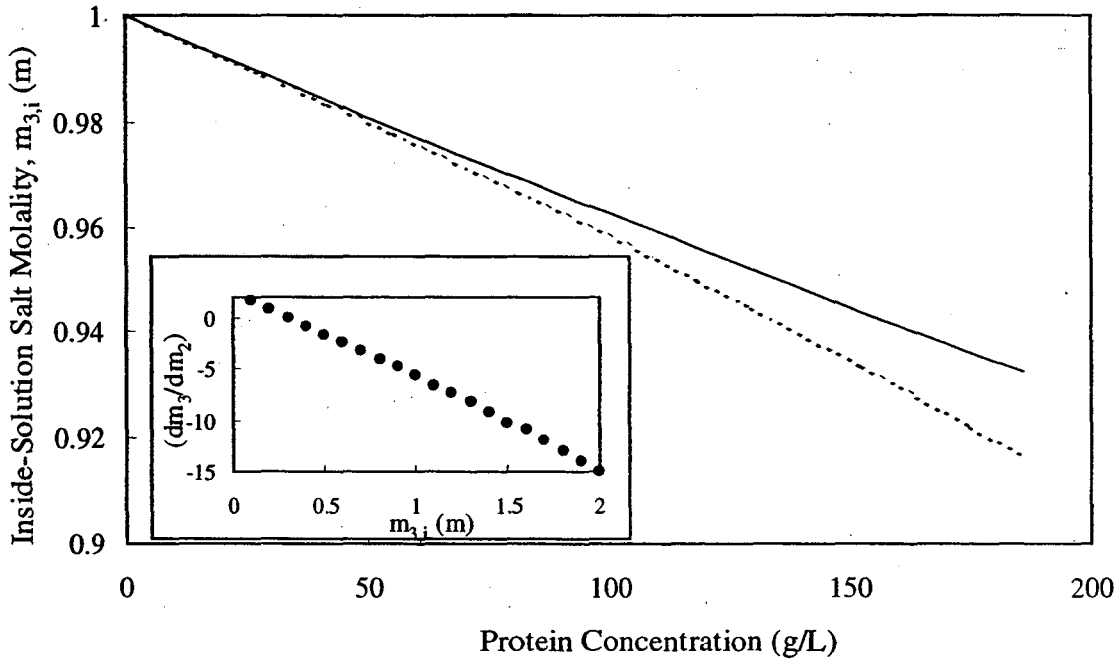
Inside-Solution Salt Molality, $m_{3,i}$ (m)
1
0.98
0.96
0.94
0.92
0.9
0
50
100
150
200
Protein Concentration (g/L)
(dm_3/dm_2)
0
-5
-10
-15
0
0.5
1
1.5
2
$m_{3,i}$ (m)

Figure iii

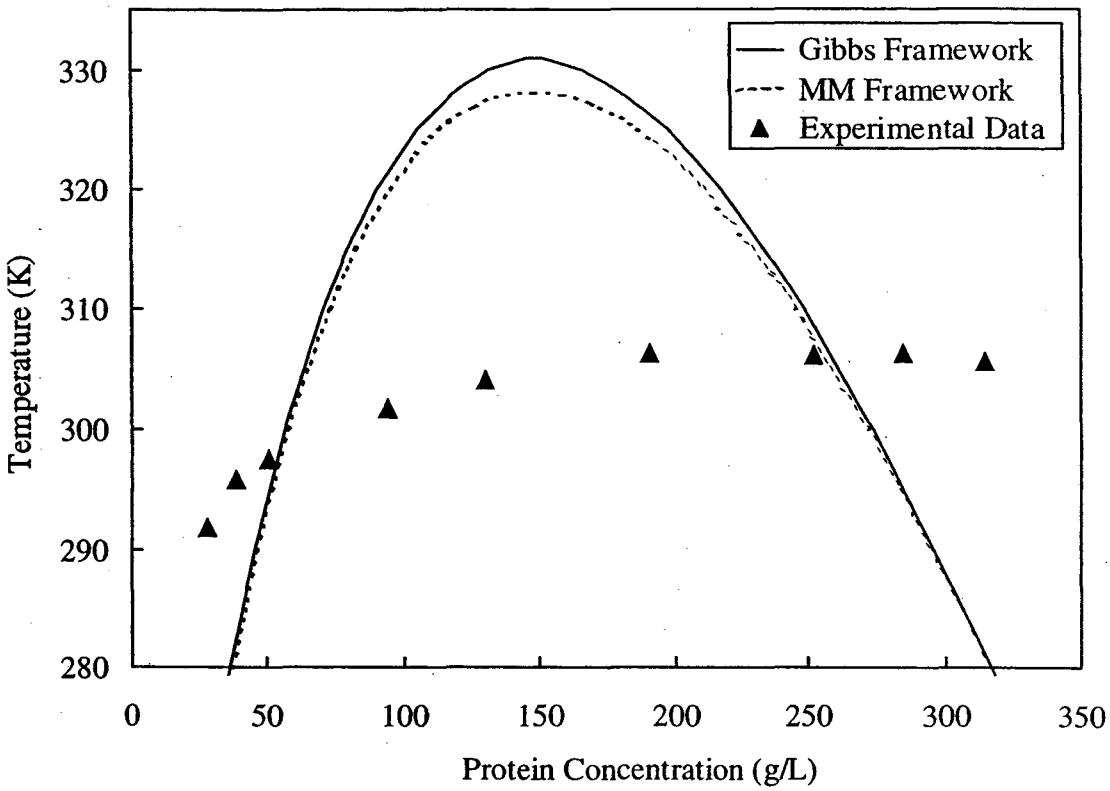
Gibbs Framework
MM Framework
Experimental Data
Temperature (K)
330
320
310
300
290
280
0
50
100
150
200
250
300
350
Protein Concentration (g/L)

Figure iv

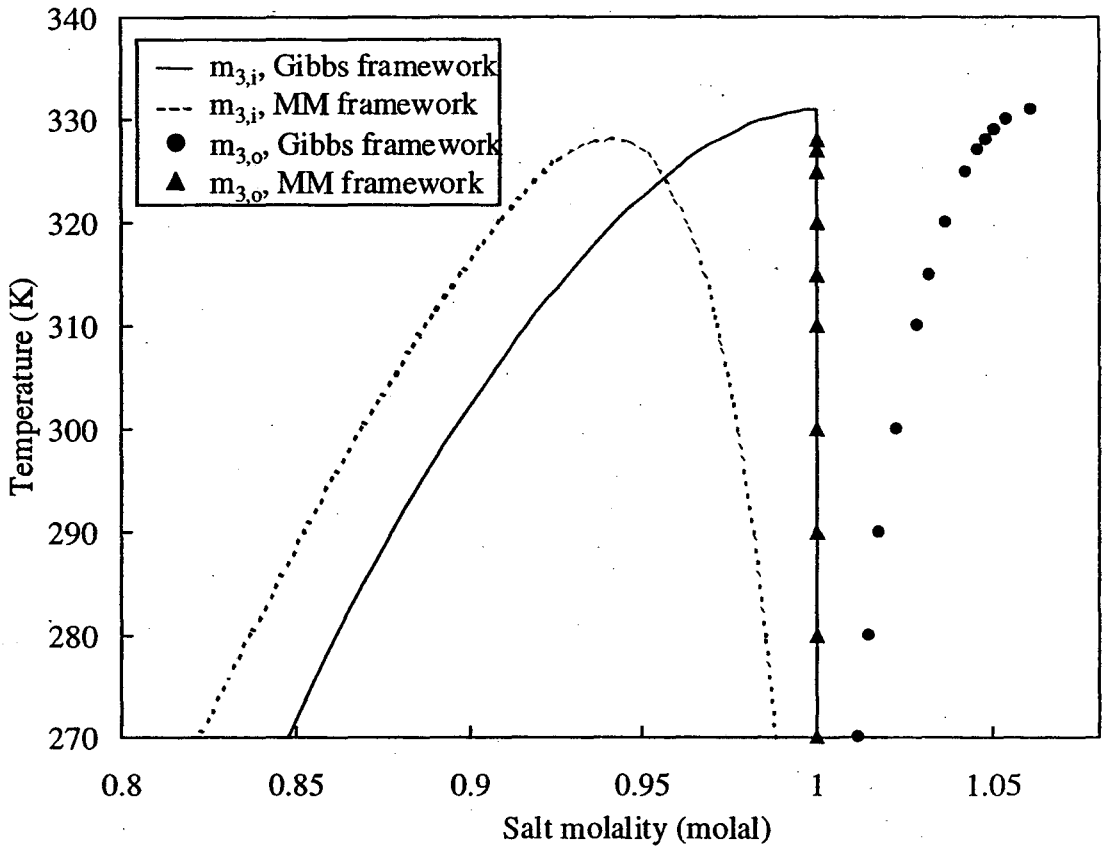
340
330
320
310
300
290
280
270
Temperature (K)
0.8
0.85
0.9
0.95
1
1.05
Salt molality (molal)
$m_{3,i}$, Gibbs framework
$m_{3,i}$, MM framework
$m_{3,o}$, Gibbs framework
$m_{3,o}$, MM framework

Figure v

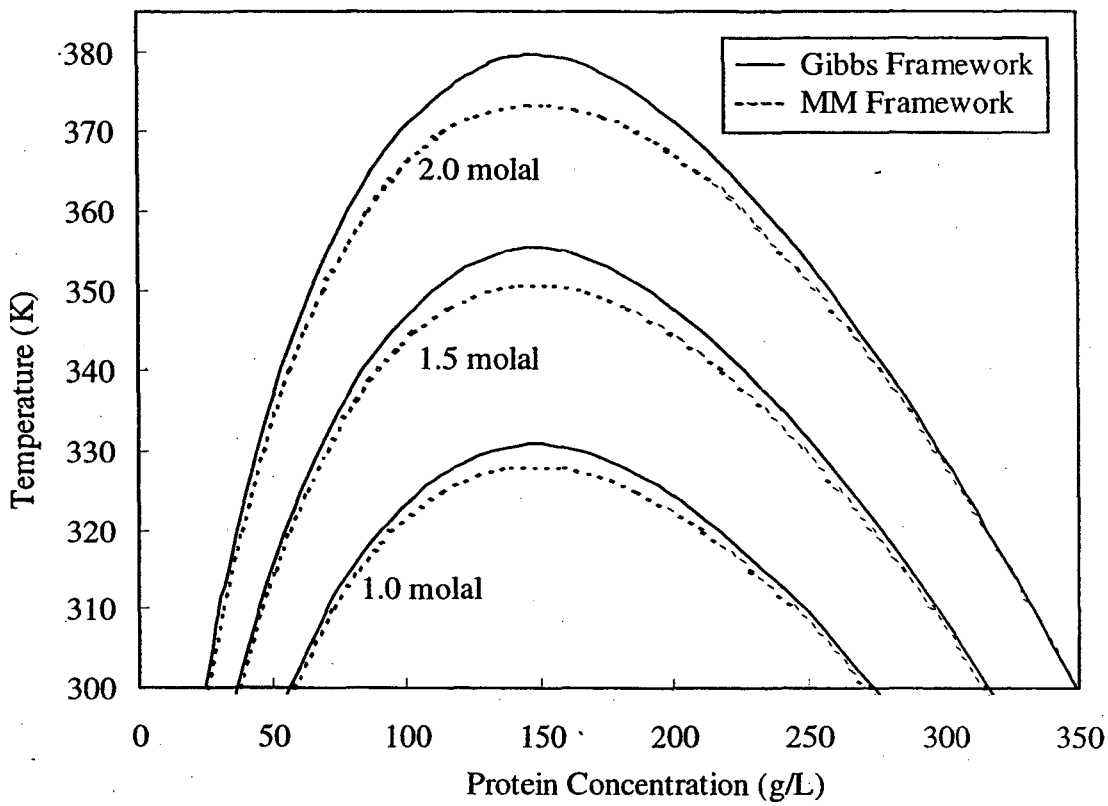
Gibbs Framework
MM Framework
2.0 molal
1.5 molal
1.0 molal
Temperature (K)
380
370
360
350
340
330
320
310
300
0
50
100
150
200
250
300
350
Protein Concentration (g/L)

Figure vi

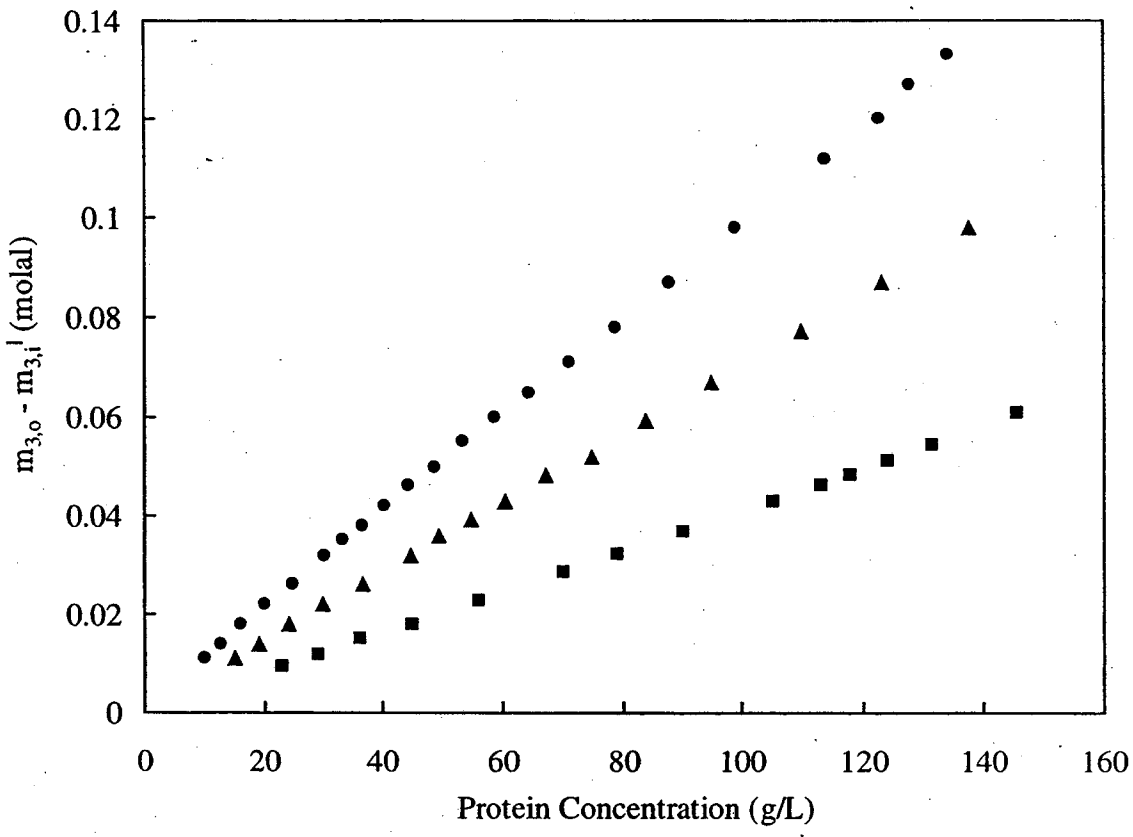
0.14
0.12
0.1
0.08
0.06
0.04
0.02
0
$m_{3,o} - m_{3,i}^{I}$ (molal)
0
20
40
60
80
100
120
140
160
Protein Concentration (g/L)

Figure vii

Ernest Orlando Lawrence Berkeley National Laboratory
One Cyclotron Road | Berkeley, California 94720

Prepared for the U.S. Department of Energy under Contract No. DE-AC03-76SF00098